


# Unconventional photon blockade in the two-photon Jaynes-Cummings model with two-frequencycavity drivings and atom driving

Xin Liu(刘欣), Meng-Yu Tian(田梦雨), Xiao-Ning Cui(崔晓宁), and Xin-He Zhang(张馨鹤)

**Citation:**CChin. Phys. B, 2024, 33 (**2**): 020308. DOI: 10.1088/1674-1056/ad0cca
Journal homepage: http://cpb.iphy.ac.cn; http://iopscience.iop.org/cpb

**What follows is a list of articles you may be interested in**

---

## Generation of microwave photon perfect *W* states of three coupled superconducting resonators

Xin-Ke Li(李新克), Yuan Zhou(周原), Guang-Hui Wang(王光辉), Dong-Yan Lv(吕东燕),Fazal Badshah, and Hai-Ming Huang(黄海铭)

Chin. Phys. B, 2023, 32 (**4**): 040306. DOI: 10.1088/1674-1056/aca394

## Photon blockade in a cavity-atom optomechanical system

Zhong Ding(丁忠) and Yong Zhang(张勇)

Chin. Phys. B, 2022, 31 (**7**): 070304. DOI: 10.1088/1674-1056/ac4cbc

## Unconventional photon blockade in a three-mode system with double second-order nonlinear coupling

Hong-Yu Lin(林宏宇), Hui Yang(杨慧), and Zhi-Hai Yao(姚治海)

Chin. Phys. B, 2020, 29 (**12**): 120304. DOI: 10.1088/1674-1056/abab82

## Decoy-state reference-frame-independent quantum key distribution with both source errors and statistical fluctuations

Kang Liu(刘康), Jian Li(李剑), Jian-Rong Zhu(朱建荣), Chun-Mei Zhang(张春梅), Qin Wang(王琴)

Chin. Phys. B, 2017, 26 (**12**): 120302. DOI: 10.1088/1674-1056/26/12/120302

## A long-distance quantum key distribution scheme based on pre-detection of optical pulse with auxiliary state

Quan Dong-Xiao (权东晓), Zhu Chang-Hua (朱畅华), Liu Shi-Quan (刘世全), Pei Chang-Xing (裴昌幸)

Chin. Phys. B, 2015, 24 (**5**): 050309. DOI: 10.1088/1674-1056/24/5/050309

---

# Unconventional photon blockade in the two-photon Jaynes–Cummings model with two-frequency cavity drivings and atom driving

Xin Liu(刘欣)[1,†], Meng-Yu Tian(田梦雨)[2], Xiao-Ning Cui(崔晓宁)[1], and Xin-He Zhang(张馨鹤)[1]

[1] *School of Physics and Technology, University of Jinan, Jinan* 250022, *China*

[2] *Marketing Service Center (Center of Metrology), State Grid ShanDong Electric Power Company, Jinan* 250001, *China*

(Received 9 September 2023; revised manuscript received 31 October 2023; accepted manuscript online 16 November 2023)

In a two-frequency cavity driving and atom driving atom-cavity system, we find the photon blockade effect. In a truncated eigenstates space, we calculate the zero-delay second-order correlation function of the cavity mode analytically and obtain an optimal condition for the photon blockade. By including three transition pathways, we find that higher excitations of the cavity mode can be further suppressed and the zero-delay second-order correlation function can be reduced additionally. Based on the master equation, we simulate the system evolution and find that the analytical solutions match well with the numerical results. Our scheme is robust with small fluctuations of parameters and may be used as a new type of single photon source.

**Keywords:** photon blockade, single photon source, quantum interference

**PACS:** 03.67.–a, 42.50.–p, 42.50.Dv **DOI:** 10.1088/1674-1056/ad0cca

## 1. Introduction

Single photon is an important resource in secure quantum key distribution,[1] quantum network,[2] and quantum computation.[3] In decades, great efforts have been devoted to generation of single photons, including parametric driven nonlinear media[4–6] and manipulation of single trapped quantum emitter.[7–9] Among these methods, single photon source based on photon blockade (PB) is an promising approach, which get great advantage both in theories and experiments.[10–21] Proposes in circuit-QED systems,[22] Kerr-type nonlinear cavities,[23] and optomechanical systems[24] have been developed and experimentally demonstrated.[25–27] A PB based single photon source is usually divided into three types: conventional photon blockade (CPB), which emerges due to the nonlinearity of the system eigenvalues,[13] unconventional photon blockade (UPB), which occurs due to destructive interferences between different transition pathways,[28] and photon blockade induced by truncation of Hilbert space, as observed in quantum linear scissors.[29] UPB was found first by Liew and Savona,[30,31] and has been studied in a optical cavity with a quantum dot,[32,33] weakly nonlinear photonicmolecules,[34] coupled optomechanical systems,[35] coupled cavities with second-order nonlinearity,[36] coupled cavities with third-order nonlinearity,[37] spinning anharmonic resonator.[38] Recently, UPB in two-photon transition processes have triggered much attention,[39–42] and other multi-photon processes have been discovered in these processes.[43] In this work, we study a system of two-photon Jaynes–Cummings model with two-frequency cavity drivings and atom driving. It is found that by setting the driving strengths properly, the photons in the cavity mode exhibit antibunching property. The zero-delay second-order correlation function is $g^{(2)}(0) \approx 0.05$, which is lower than that in Ref. [42]. Analytical and numerical results reveal that antibunching phenomena are due to interference between different transition pathways. Smooth variations of $g^{(2)}(0)$ with variations of driving strengths manifest that these UPB phenomena are robust with small fluctuations of driving strengths.

The rest of the paper is organized as follows. In Section 2, we introduce the setup and Hamiltonian of the system. In Section 3, we analytically calculate the expression of the zero-delay second-order correlation function and obtain an optimal condition for the photon blockade. Numerical simulation and discussion of experimental feasibility are present in Section 4 with a brief conclusion in Section 5.

## 2. Setup and model

We consider a setup composed of a cavity coupled to a two-level atom via a two-photon interaction, with the cavity driven by laser of frequency $\omega_r$ and laser of frequency $2\omega_r$ and the atom driven by laser of frequency $\omega_q$ as illustrated in Fig. 1(a). The system Hamiltonian reads (hereafter $\hbar = 1$)

$$\begin{aligned} H = {} & \omega_r a^\dagger a + \frac{\omega_q}{2}\sigma_z + g(a^{\dagger 2}\sigma_- + a^2\sigma_+) \\ & + \frac{E}{2}(a^\dagger \mathrm{e}^{-\mathrm{i}\omega_r t} + a\,\mathrm{e}^{\mathrm{i}\omega_r t}) \\ & + \frac{F}{2}(a^{\dagger 2}\mathrm{e}^{-2\mathrm{i}\omega_r t}\mathrm{e}^{\mathrm{i}\theta} + a^2\mathrm{e}^{2\mathrm{i}\omega_r t}\mathrm{e}^{-\mathrm{i}\theta}) \end{aligned}$$

†Corresponding author. E-mail: sps_liux@ujn.edu.cn

© 2024 Chinese Physical Society and IOP Publishing Ltd 

$$+\frac{\Omega}{2}(\sigma_+ e^{-i\omega_q t} e^{i\varphi} + \sigma_- e^{i\omega_q t} e^{-i\varphi}), \quad (1)$$

where $a^\dagger$ and $a$ denote the creation and annihilation operators of the cavity mode of frequency $\omega_r$; $\sigma_+$ and $\sigma_-$ denote the rasing and lowering operators of the two-level atom with an energy separation of $\omega_q$ between the excited state $|e\rangle$ and the ground state $|g\rangle$. The third term represents the two-photon interaction between the cavity mode and the atom with interaction strength $g$. The cavity is driven by a laser of frequency $\omega_r$ with strength $E/2$ and a laser of frequency $2\omega_r$ with strength $F/2$ and phase difference $\theta$ compared to the first laser, which can be implemented by a second-order nonlinearity process.[42] The atom is driven by another laser of frequency $\omega_q$ with strength $\Omega/2$ and phase difference $\varphi$ compared to the first laser. We choose the frequencies of the cavity and the atom in a two-photon resonant case, i.e., $\omega_q = 2\omega_r$. Thus, the Hamiltonian in the interaction picture reads

$$\begin{aligned} H_{\rm I} =& g(a^{\dagger 2}\sigma_- + a^2\sigma_+) \\ &+ \frac{E}{2}(a^\dagger + a) + \frac{F}{2}(a^{\dagger 2} e^{i\theta} + a^2 e^{-i\theta}) \\ &+ \frac{\Omega}{2}(\sigma_+ e^{i\varphi} + \sigma_- e^{-i\varphi}). \end{aligned} \quad (2)$$

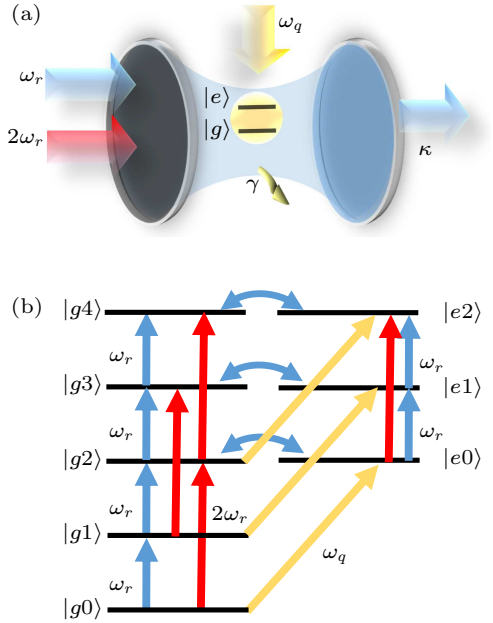



**Fig. 1.** (a) Schematic of the setup considered, which consists of a cavity coupled to a two-level atom via a two-photon interaction, with the cavity driven by laser of frequency $\omega_r$ and laser of frequency $2\omega_r$ and the atom driven by laser of frequency $\omega_q$. The cavity decays with rate $\kappa$ and the atom decays with rate $\gamma$. (b) Eight lowest bare-state energy levels of the system and their transition pathways.

We consider the weak driving and bad cavity case, i.e., $\kappa \gg F,\ E,\ \Omega,\ g$. In this situation the higher states are rarely populated, so we can only consider the lowest energy levels. In Fig. 1(b), eight lowest bare-state energy levels of the system and their transition pathways are depicted. When the transition pathways $|g0\rangle \to |g1\rangle \to |g2\rangle$, $|g0\rangle \to |g2\rangle$, and $|g0\rangle \to |e0\rangle \to |g2\rangle$ destructively interfere, the two-photon state $|g2\rangle$ cannot be occupied and the unconventional photon blockade occurs. To evaluate the strength of the unconventional photon blockade and the purity of single photons, the zero-delay second-order correlation function $g^{(2)}(0) = \langle a^\dagger a^\dagger a a\rangle / \langle a^\dagger a\rangle^2$ in steady state is usually used. When $g^{(2)}(0) \ll 1$, the photons are antibunching and a single-photon source is realized.

## 3. Analytical expression of zero-delay second-order correlation function

To obtain an analytical expression of the zero-delay second-order correlation function, we introduce the non-Hermite Hamiltonian

$$\begin{aligned} \widetilde{H} =& g(a^{\dagger 2}\sigma_- + a^2\sigma_+) \\ &+ \frac{E}{2}(a^\dagger + a) + \frac{F}{2}(a^{\dagger 2} e^{i\theta} + a^2 e^{-i\theta}) \\ &+ \frac{\Omega}{2}(\sigma_+ e^{i\varphi} + \sigma_- e^{-i\varphi}) - \frac{i}{2}\kappa a^\dagger a - \frac{i}{2}\gamma\sigma_+\sigma_- \end{aligned} \quad (3)$$

to include the influence of the dissipations of the cavity mode and the atom, where $\kappa$ is the decay rate of the cavity mode and $\gamma$ is the decay rate of the atom. Under the weak driving assumption, we expand the system state with the eight lowest states as

$$\begin{aligned} |\psi(t)\rangle =& C_1(t)|g0\rangle + C_2(t)|g1\rangle + C_3(t)|g2\rangle + C_4(t)|e0\rangle \\ &+ C_5(t)|g3\rangle + C_6(t)|e1\rangle + C_7(t)|g4\rangle + C_8(t)|e2\rangle. \end{aligned} \quad (4)$$

Depending on the Schrödinger equation $i\partial|\psi(t)\rangle/\partial t = \widetilde{H}|\psi(t)\rangle$, we obtain the equations of motion of these probability amplitudes $C_i(t)$ as

$$i\dot{C}_1(t) = \frac{E}{2}C_2(t) + \frac{F}{\sqrt{2}}e^{-i\theta}C_3(t) + \frac{\Omega}{2}e^{-i\varphi}C_4(t), \quad (5)$$

$$i\dot{C}_2(t) = \frac{E}{2}C_1(t) + \frac{E}{\sqrt{2}}C_3(t) - \frac{i}{2}\kappa C_2(t), \quad (6)$$

$$\begin{aligned} i\dot{C}_3(t) =& \sqrt{2}gC_4(t) + \frac{E}{\sqrt{2}}C_2(t) + \frac{F}{\sqrt{2}}e^{i\theta}C_1(t) \\ &+ \sqrt{3}F e^{-i\theta}C_7(t) + \frac{\Omega}{2}e^{-i\varphi}C_8(t) - i\kappa C_3(t), \end{aligned} \quad (7)$$

$$\begin{aligned} i\dot{C}_4(t) =& \sqrt{2}gC_3(t) + \frac{\Omega}{2}e^{i\varphi}C_1(t) \\ &+ \frac{\sqrt{2}}{2}F e^{-i\theta}C_8(t) - \frac{i}{2}\gamma C_4(t), \end{aligned} \quad (8)$$

$$\begin{aligned} i\dot{C}_5(t) =& \sqrt{6}gC_6(t) + \frac{\sqrt{3}}{2}EC_3(t) + \frac{\sqrt{6}}{2}F e^{i\theta}C_2(t) \\ &+ EC_7(t) - \frac{3}{2}i\kappa C_5(t), \end{aligned} \quad (9)$$

$$\begin{aligned} i\dot{C}_6(t) =& \sqrt{6}gC_5(t) + \frac{E}{2}C_4(t) + \frac{\Omega}{2}e^{i\varphi}C_2(t) \\ &+ \frac{\sqrt{2}}{2}EC_8(t) - \frac{i}{2}\kappa C_6(t) - \frac{i}{2}\gamma C_6(t), \end{aligned} \quad (10)$$

$$\begin{aligned} i\dot{C}_7(t) =& EC_5(t) + \sqrt{3}F e^{i\theta}C_3(t) \\ &+ 2\sqrt{3}gC_8(t) - 2i\kappa C_7(t), \end{aligned} \quad (11)$$

$$\mathrm{i}\dot{C}_8(t) = \frac{\sqrt{2}}{2}EC_6(t) + \frac{\sqrt{2}}{2}F\,\mathrm{e}^{\mathrm{i}\theta}C_4(t) + \frac{\Omega}{2}\,\mathrm{e}^{\mathrm{i}\varphi}C_3(t) + 2\sqrt{3}gC_7(t) - \mathrm{i}\kappa C_8(t) - \frac{\mathrm{i}}{2}\gamma C_8(t). \tag{12}$$

Under the weak driving condition, the probability amplitudes scale as $C_1(t) \gg \{C_2(t), C_4(t)\} \gg \{C_3(t), C_6(t)\} \gg C_5(t), C_8(t) \gg C_7(t)$. The equations of motion for $C_i(t)$ can be approximately solved by a perturbation method, i.e., discard the higher-order terms in the equations of motion for the lower-order variables. By assuming $C_1(t) = 1$, the steady-state solutions of the probability amplitudes can be obtained by setting $\partial C_i(t)/\partial t = 0$ as

$$C_1 = 1, \tag{13}$$

$$C_2 = \frac{E}{\mathrm{i}\kappa}, \tag{14}$$

$$C_3 = \frac{\sqrt{2}\mathrm{i}\kappa(2\mathrm{i}g\Omega\,\mathrm{e}^{\mathrm{i}\varphi} - F\gamma\mathrm{e}^{\mathrm{i}\theta}) - \sqrt{2}E^2\gamma}{2\kappa(4g^2 + \kappa\gamma)}, \tag{15}$$

$$C_4 = \frac{1}{\mathrm{i}\gamma}\Big[\Omega\,\mathrm{e}^{\mathrm{i}\varphi} - \frac{4g^2\kappa\Omega\,\mathrm{e}^{\mathrm{i}\varphi} + 2gE^2\gamma + \mathrm{i}2g\kappa\gamma F\,\mathrm{e}^{\mathrm{i}\theta}}{\kappa(4g^2 + \kappa\gamma)}\Big], \tag{16}$$

$$C_5 = \frac{\mathrm{i}E\{E^2[-8g^2 + \gamma(\gamma+\kappa)] + [8g^2 + 3\kappa(\gamma+\kappa)](\mathrm{i}\,\mathrm{e}^{\mathrm{i}\theta}F\gamma + 2\mathrm{e}^{\mathrm{i}\varphi}g\Omega)\}}{\sqrt{6}\kappa(4g^2 + \gamma\kappa)[8g^2 + \kappa(\gamma+\kappa)]}, \tag{17}$$

$$C_6 = \frac{E\{2E^2g(\gamma+\kappa) + 2\mathrm{i}\,\mathrm{e}^{\mathrm{i}\theta}Fg[8g^2 + \kappa(3\gamma+\kappa)] - \mathrm{e}^{\mathrm{i}\varphi}\kappa^2(\gamma+\kappa)\Omega\}}{\kappa(4g^2 + \gamma\kappa)(8g^2 + \kappa(\gamma+\kappa))}, \tag{18}$$

$$\begin{aligned} C_7 = {} & \frac{E^4[\gamma(\gamma+\kappa)(\gamma+2\kappa) - 8g^2(4\gamma+5\kappa)] - 2\mathrm{i}E^2F\,\mathrm{e}^{\mathrm{i}\theta}[-3\gamma\kappa(\gamma+\kappa)(\gamma+2\kappa) + 192g^4 + 8g^2(-2\gamma^2 + 2\gamma\kappa + 3\kappa^2)]}{2\sqrt{6}\kappa^2(\gamma+2\kappa)(\gamma\kappa+4g^2)[\kappa(\gamma+\kappa)+8g^2]} \\ & + \frac{4E^2g\,\mathrm{e}^{\mathrm{i}\varphi}\Omega[3\kappa(\gamma+\kappa)(\gamma+2\kappa) + 8g^2(2\gamma+\kappa)] - 3F^2\,\mathrm{e}^{2\mathrm{i}\theta}\kappa[\kappa(\gamma+\kappa)+8g^2][\gamma(\gamma+2\kappa) - 8g^2]}{2\sqrt{6}\kappa^2(\gamma+2\kappa)(\gamma\kappa+4g^2)[\kappa(\gamma+\kappa)+8g^2]} \\ & + \frac{12\mathrm{i}Fg\kappa\Omega(\gamma+2\kappa)\,\mathrm{e}^{\mathrm{i}(\theta+\varphi)}(\kappa(\gamma+\kappa)+8g^2) + 12g^2\kappa\mathrm{e}^{2\mathrm{i}\varphi}\Omega^2[\kappa(\gamma+\kappa)+8g^2]}{2\sqrt{6}\kappa^2(\gamma+2\kappa)(\gamma\kappa+4g^2)[\kappa(\gamma+\kappa)+8g^2]}, \end{aligned} \tag{19}$$

$$\begin{aligned} C_8 = {} & \frac{-4\mathrm{i}E^4g(\gamma+\kappa) + 8E^2Fg\,\mathrm{e}^{\mathrm{i}\theta}[\kappa(2\gamma+\kappa)+8g^2] + \mathrm{i}E^2\,\mathrm{e}^{\mathrm{i}\varphi}\Omega(\kappa(\gamma+\kappa)(\gamma+2\kappa)+8\gamma g^2)}{\sqrt{2}\kappa(\gamma+2\kappa)(\gamma\kappa+4g^2)[\kappa(\gamma+\kappa)+8g^2]} \\ & + \frac{4\mathrm{i}F^2g\,\mathrm{e}^{2\mathrm{i}\theta}\kappa[\kappa(\gamma+\kappa)+8g^2] - F\kappa\Omega(\gamma+2\kappa)\,\mathrm{e}^{\mathrm{i}(\theta+\varphi)}[\kappa(\gamma+\kappa)+8g^2] + 2\mathrm{i}g\kappa\,\mathrm{e}^{2\mathrm{i}\varphi}\Omega^2[\kappa(\gamma+\kappa)+8g^2]}{\sqrt{2}\kappa(\gamma+2\kappa)(\gamma\kappa+4g^2)[\kappa(\gamma+\kappa)+8g^2]}. \end{aligned} \tag{20}$$

The zero-delay second-order correlation function of cavity mode approximates to

$$g^{(2)}(0) = \frac{\langle a^\dagger a^\dagger aa\rangle}{\langle a^\dagger a\rangle^2} \approx \frac{2P_2}{(P_1+2P_2)^2} \approx \frac{2P_2}{P_1^2} \approx \frac{2|C_3|^2}{|C_2|^4}, \tag{21}$$

where the $n$-photon probabilities are

$$P_1 = \frac{|C_2|^2}{|C_1|^2 + |C_2|^2 + |C_3|^2 + |C_4|^2}, \tag{22}$$

$$P_2 = \frac{|C_3|^2}{|C_1|^2 + |C_2|^2 + |C_3|^2 + |C_4|^2}. \tag{23}$$

A case corresponding to a perfect photon blockade is $C_3 = 0$, which means that there is no two-photon probability in the cavity mode. A further suppression of the multi-photon excitation could be realized by minimizing the probability amplitude $C_5$ of state $|g3\rangle$. Unfortunately, the probability amplitudes $C_3$ and $C_5$ cannot be zero simultaneously due to the same component $2\mathrm{i}g\Omega\,\mathrm{e}^{\mathrm{i}\varphi} - F\gamma\mathrm{e}^{\mathrm{i}\theta}$. To reduce $C_7$ and $C_8$ under the condition $C_3 = 0$, the two parts arising from the high frequency driving of cavity mode and driving of atom should have opposite symbols. Without loss of generality, we choose $\theta = \pi/2$, $\varphi = 0$, thus an optimal parameter condition can be obtained as

$$2g\kappa\Omega + E^2\gamma - \kappa\gamma F = 0. \tag{24}$$

## 4. Simulation and discussion

To verify our analytical results, we perform numerical simulation base on a master equation method. Assuming that the cavity and the atom are connected with two individual vacuum baths, the system evolution is governed by the master equation

$$\begin{aligned} \frac{\mathrm{d}\rho(t)}{\mathrm{d}t} = {} & \mathrm{i}[\rho(t), H_\mathrm{I}] + \tfrac{\kappa}{2}[2a\rho(t)a^\dagger - a^\dagger a\rho(t) - \rho(t)a^\dagger a] \\ & + \tfrac{\gamma}{2}[2\sigma_-\rho(t)\sigma_+ - \sigma_+\sigma_-\rho(t) - \rho(t)\sigma_+\sigma_-], \end{aligned} \tag{25}$$

where $\kappa$ ($\gamma$) is the decay rate of the cavity (atom). By solving Eq. (25) numerically, a steady state density matrix $\rho_\mathrm{ss}$ is obtained and the zero-delay second-order correlation function is calculated as $g^{(2)}(0) = \mathrm{Tr}[a^\dagger a^\dagger aa\rho_\mathrm{ss}]/(\mathrm{Tr}[a^\dagger a\rho_\mathrm{ss}])^2$. In the same way, we can calculate occupied probability of each state as $|C_i|^2 = \mathrm{Tr}[|j\rangle\langle j|\rho_\mathrm{ss}]$ for $|j\rangle$ representing $|g0\rangle$, $|g1\rangle$, $|g2\rangle$, $|e0\rangle$, $|g3\rangle$, $|e2\rangle$, $|g4\rangle$ or $|e2\rangle$. The average photon number of the cavity mode can also be calculated as $\bar{n} = \mathrm{Tr}[a^\dagger a\rho_\mathrm{ss}]$.

In our simulation, we truncated the photon number states space up to five photons under the weak driving assumption and the parameters are chosen to be $\omega_q = 2\omega_r = 8\times 2\pi$ GHz, $g = 0.01\omega_r$, $F = 0.36g$, $\Omega = 10g$, $\theta = \pi/2$, $\varphi = 0$, $\kappa = \gamma =$

$100g$, $E$ varies between 0 and $20g$. In Fig. 2(a), we plot the occupied probabilities of the lowest eight states as functions of the driving strength $E$. It is verified that the probability amplitudes obey $C_1 \approx 1$ and $C_1 \gg \{C_2, C_4\} \gg \{C_3, C_6\} \gg \{C_5, C_8\} \gg C_7$. The occupied probabilities $|C_2|^2$, $|C_6|^2$ increase with the increase of driving strength $E$. $|C_4|^2$ depends on the driving strength $\Omega$ and the atom decay rate $\gamma$. $|C_5|^2$ cannot be suppressed under the condition $C_3 = 0$. $|C_7|^2$ and $|C_8|^2$ are partly suppressed as shown in the figure by small dips of the lines. In Fig. 2(b), we plot the correlation function $g^{(2)}(0)$ and the average photon number $\langle a^\dagger a \rangle$ of the cavity mode as functions of the driving strength $E$. The red dotted line is $g^{(2)}(0)$ with cavity mode driven by lasers of two frequencies and without atom driving. The dot-dashed line is $g^{(2)}(0)$ with atom driving and low frequency cavity driving. The solid line is $g^{(2)}(0)$ with three drivings. It can be found that three transition pathways have effect on suppressing higher excitations. There is a dip of $g^{(2)}(0) \approx 0.05$ at a value of $E$ determined by Eq. (24). The dip of $g^{(2)}(0)$ is at the same value of $E$ with the dip of occupied probability $|C_3|^2$, which indicates that the optimal photon blockade occurs due to the quantum interference of different transition pathways. The inset in Fig. 2(b) describes the increase of the average photon number $\langle a^\dagger a \rangle$ with the increase of the driving strength $E$ as a natural result.

To verify the optimal condition for the photon blockade, i.e., Eq. (24) and photon blockade robustness with parameter fluctuations, we plot the $g^{(2)}(0)$ as functions of $E$, $F$, and $\Omega$ in Fig. 3. The black dashed lines indicate the optimal condition of the photon blockade determined by Eq. (24). In Figs. 3(a)–3(c), the lines of optimal condition match well with the numerical results obtained by the master equation in most of the region. The higher $g^{(2)}(0)$ in some regions with very small driving strengths are due to the constant strength of the third driving, which induces a bunching effect of the photons in the cavity mode. The simulations indicate that the photon blockade in our system is robust with small parameter fluctuations.

Our proposal can be implemented in a superconducting quantum circuit, which can realize a coupling strength $g = 0.01\omega_r = 40 \times 2\pi$ MHz.[40] The frequency of a transmission-line resonator can vary between $1 \times 2\pi$ GHz to $10 \times 2\pi$ GHz.[44] The superconducting qubit acting as a two-level atom can be addressed and driven individually by microwave. A large decay rate of the cavity mode can be realized by designing of coupling inductance,[45] and a Hanbury–Brown–Twiss test of the quantum correlation of emitted photons can be realized by measuring the moments of the two quadratures.[46] Our scheme can also be implemented by a Fabry–Pérot cavity as described in Ref. [47].

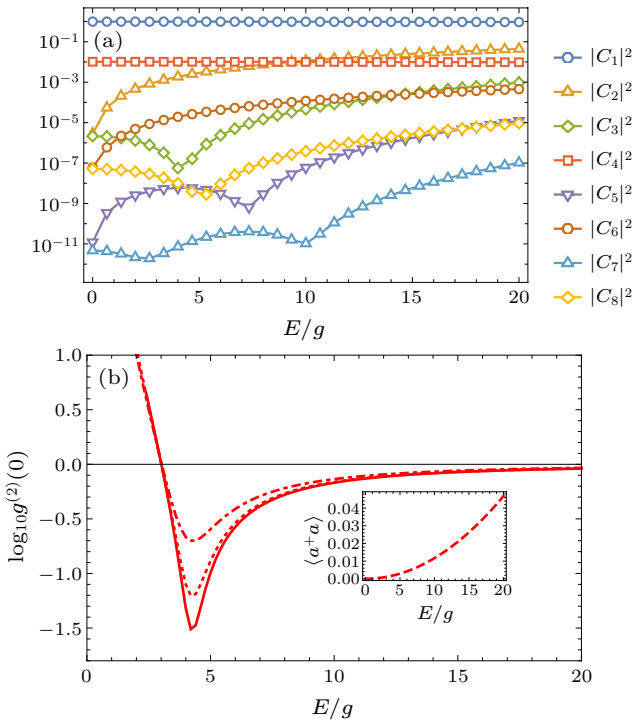



**Fig. 2.** (a) The occupied probabilities of states $|C_i|^2$ versus the driving strength $E$. (b) The zero-decay second-order correlation function $g^{(2)}(0)$ versus the driving strength $E$. The dotted line is $g^{(2)}(0)$ without atom driving, the dot-dashed line is $g^{(2)}(0)$ without high frequency cavity driving and the solid line is $g^{(2)}(0)$ with two-frequency cavity drivings and atom driving. The inset is the average photon number $\langle a^\dagger a \rangle$ versus the driving strength $E$. The parameters are $\omega_q = 2\omega_r = 8 \times 2\pi$ GHz, $g = 0.01\omega_r$, $F = 0.36g$, $\Omega = 10g$, $\theta = \pi/2$, $\varphi = 0$, and $\kappa = \gamma = 100g$.

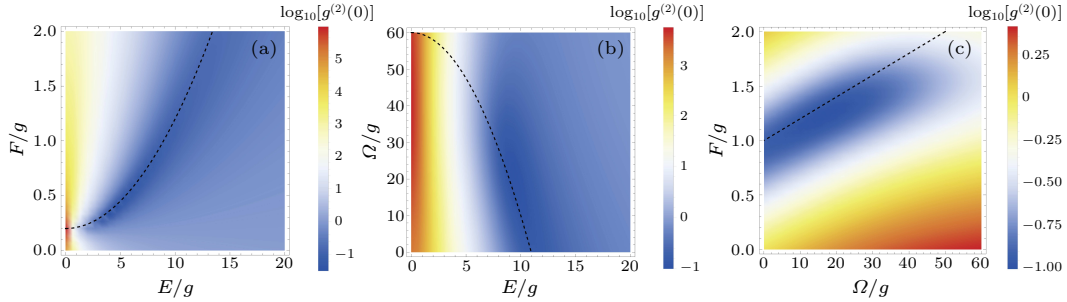



**Fig. 3.** (a) The $g^{(2)}(0)$ versus the driving strength $F$ and $E$. The other parameters are $\omega_q = 2\omega_r = 8 \times 2\pi$ GHz, $g = 0.01\omega_r$, $\Omega = 10g$, $\theta = \pi/2$, $\varphi = 0$, and $\kappa = \gamma = 100g$. (b) The $g^{(2)}(0)$ versus the driving strength $\Omega$ and $E$. The other parameters are $\omega_q = 2\omega_r = 8 \times 2\pi$ GHz, $g = 0.01\omega_r$, $F = 1.2g$, $\theta = \pi/2$, $\varphi = 0$, and $\kappa = \gamma = 100g$. (c) The $g^{(2)}(0)$ versus the driving strength $F$ and $\Omega$. The other parameters are $\omega_q = 2\omega_r = 8 \times 2\pi$ GHz, $g = 0.01\omega_r$, $E = 10g$, $\theta = \pi/2$, $\varphi = 0$, and $\kappa = \gamma = 100g$. The black lines indicate the optimal condition determined by Eq. (24).

## 5. Conclusion

In summary, we have studied a system consisting of an atom coupled to a cavity with two-photon interaction. By choosing proper strength of atom driving and strengths of two-frequency cavity drivings, a prominent photon blockade can be obtained. We have analytically calculated the optimal condition for the photon blockade and found that three transition pathways can further reduce the zero-delay second-order correlation function compared with the cases of two transition pathways. Analytical results match well with the numerical results obtained by the master equation. The numerical results also reveal that the photon blockade in this system is robust against small fluctuations of parameters. The system can act as a single photon source.

## Acknowledgment

Project supported by the National Natural Science Foundation of China (Grant No. 61601196).

## References

[1] Shor P W and Preskill J 2000 *Phys. Rev. Lett.* **85** 441
[2] Brekenfeld M, Niemietz D, Christesen J D and Rempe G 2020 *Nat. Phys.* **16** 647
[3] Steane A 1998 *Rep. Prog. Phys.* **61** 117
[4] Goldschmidt E A, Eisaman M D, Fan J, Polyakov S V and Migdall A 2008 *Phys. Rev. A* **78** 013844
[5] Ma X S, Zotter S, Kofler J, Jennewein T and Zeilinger A 2011 *Phys. Rev. A* **83** 043814
[6] Yuan C H, Chen L Q, Ou Z Y and Zhang W 2011 *Phys. Rev. A* **83** 054302
[7] McKeever J, Boca A, Boozer A D, Miller R, Buck J R, Kuzmich A and Kimble H J 2004 *Science* **303** 1992
[8] Darquié B, Jones M P, Dingjan J, Beugnon J, Bergamini S, Sortais Y, Messin G, Browaeys A and Grangier P 2005 *Science* **309** 454
[9] Hennrich M, Legero T, Kuhn A and Rempe G 2004 *New J. Phys.* **6** 86
[10] Gerace D and Savona V 2014 *Phys. Rev. A* **89** 031803
[11] Zhou Y H, Shen H Z and Yi X X 2015 *Phys. Rev. A* **92** 023838
[12] Shen H Z, Shang C, Zhou Y H and Yi X X 2018 *Phys. Rev. A* **98** 023856
[13] Birnbaum K M, Boca A, Miller R, Boozer A D, Northup T E and Kimble H J 2005 *Nature* **436** 87
[14] Faraon A, Fushman I, Englund D, Stoltz N, Petroff P and Vuckovic J 2008 *Nat. Phys.* **4** 859
[15] Hamsen C, Tolazzi K N, Wilk T and Rempe G 2017 *Phys. Rev. Lett.* **118** 133604
[16] Lang C, Bozyigit D, Eichler C, Steffen L, Fink J M, Abdumalikov Jr A A, Baur M, Filipp S, da Silva M P, Blais A and Wallraff A 2011 *Phys. Rev. Lett.* **106** 243601
[17] Huang R, Miranowicz A, Liao J Q, Nori F and Jing H 2018 *Phys. Rev. Lett.* **121** 153601
[18] Peyronel T, Firstenberg O, Liang Q Y, Hofferberth S, Gorshkov A V, Pohl T, Lukin M D and Vuletic V 2012 *Nature* **488** 57
[19] Ridolfo A, Leib M, Savasta S and Hartmann M J 2012 *Phys. Rev. Lett.* **109** 193602
[20] Zuo Y, Huang R, Kuang L M, Xu X W and Jing H 2022 *Phys. Rev. A* **106** 043715
[21] Vaneph C, Morvan A, Aiello G, Féchant M, Aprili M, Gabelli J and Estève J 2018 *Phys. Rev. Lett.* **121** 043602
[22] Liu Y X, Xu X W, Miranowicz A and Nori F 2014 *Phys. Rev. A* **89** 043818
[23] Ferretti S, Andreani L C, Tureci H E and Gerace D 2010 *Phys. Rev. A* **82** 013841
[24] Liao J Q and Nori F 2013 *Phys. Rev. A* **88** 023853
[25] Hoffman A J, Srinivasan S J, Schmidt S, Spietz L, Aumentado J, Tureci H E and Houck A A 2011 *Phys. Rev. Lett.* **107** 053602
[26] Snijders H J, Frey J A, Norman J, Flayac H, Savona V, Gossard A C, Bowers J E, van Exter M P, Bouwmeester D and Loffler W 2018 *Phys. Rev. Lett.* **121** 043601
[27] Trivedi R, Radulaski M, Fischer K A, Fan S and Vuckovic J 2019 *Phys. Rev. Lett.* **122** 243602
[28] Flayac H and Savona V 2017 *Phys. Rev. A* **96** 053810
[29] Lvovsky A I and Mlynek J 2002 *Phys. Rev. Lett.* **88** 250401
[30] Liew T C and Savona V 2010 *Phys. Rev. Lett.* **104** 183601
[31] Bamba M, Imamoglu A, Carusotto I and Ciuti C 2011 *Phys. Rev. A* **83** 021802
[32] Majumdar A, Bajcsy M, Rundquist A and Vuckovic J 2012 *Phys. Rev. Lett.* **108** 183601
[33] Zhang W, Yu Z, Liu Y and Peng Y 2014 *Phys. Rev. A* **89** 043832
[34] Xu X W and Li Y 2014 *Phys. Rev. A* **90** 033809
[35] Xu X W and Li Y J 2013 *J. Phys. B: At. Mol. Opt. Phys.* **46** 035502
[36] Zhou Y H, Wu Q C, Ye B, Xue L and Shen H Z 2019 *Int. J. Theor. Phys.* **58** 472
[37] Zou F, Lai D G and Liao J Q 2020 *Opt. Express* **28** 16175
[38] Li B, Huang R, Xu X, Miranowicz A and Jing H 2019 *Photon. Res.* **7** 630
[39] Felicetti S, Rossatto D Z, Rico E, Solano E and Forn-Díaz P 2018 *Phys. Rev. A* **97** 013851
[40] Zou F, Zhang X Y, Xu X W, Huang J F and Liao J Q 2020 *Phys. Rev. A* **102** 053710
[41] Li H, Zhang S Q, Guo M, Li M X and Song L J 2019 *Acta Phys. Sin.* **68** 124203 (in Chinese)
[42] Yan Y, Cheng Y, Guan S, Yu D and Duan Z 2018 *Opt. Lett.* **43** 5086
[43] Jiang S Y, Zou F, Wang Y, Huang J F, Xu X W and Liao J Q 2023 *Opt. Express* **31** 15697
[44] Liu X, Liao Q, Xu X, Fang G and Liu S 2016 *Opt. Commun.* **359** 359
[45] Yin Y, Chen Y, Sank D, O'Malley P J J, White T C, Barends R, Kelly J, Lucero E, Mariantoni M, Megrant A, Neill C, Vainsencher A, Wenner J, Korotkov A N, Cleland A N and Martinis J M 2013 *Phys. Rev. Lett.* **110** 107001
[46] Da Silva M P, Bozyigit D, Wallraff A and Blais A 2010 *Phys. Rev. A* **82** 043804
[47] Chen M, Tang J, Tang L, Wu H and Xia K 2022 *Phys. Rev. Res.* **4** 033083